phosphoric acid solution. Before distillation, the system was purged with steam and then filled with an atmosphere of the appropriate gas. The water was then distilled directly into the reaction vessel. By this method water was obtained at pH 7. To 300 ml of water purified in this fashion was added enough material for irradiation to bring the suspension or solution to 0.006 *M*. A positive flow of the saturating gas was maintained during the addition of the organic compound in order to avoid simultaneous admission of air to the apparatus. For runs in D_2O,[11] argon gas was bubbled through the D_2O in the reaction vessel for 1 hr, displacing dissolved air, prior to addition of the butanoic acid or butanal. In all runs the gaseous products were analyzed by gas chromatography. Two columns were used. Carbon dioxide and methane were analyzed on a 10 ft × $^1/_8$ in. molecular sieve column operated at ambient temperature with a 10-ml per hr nitrogen flow rate. A 12 ft × $^1/_8$ in. Porapak R column, operated at ambient temperature with a 15-ml per hr nitrogen flow, was used to analyze carbon monoxide, methane, ethane, ethylene, and acetylene. The rate of gas evolution during irradiation was followed using a gas buret. The aqueous phase in the irradiated reaction vessel was analyzed by saturating the solutions with sodium chloride and continuous extraction with diethyl ether for 16 hr. After evaporation of the ether the residues were analyzed by gas chromatography. The column utilized was a 10 ft × $^1/_8$ in. 30% DEHS operated at 150° with a 30-ml/hr helium flow rate. To examine the deuterium label in the methane product, gas samples were removed from above the irradiated solutions with a gas syringe. These samples were then admitted to the mass spectrometer and spectra taken utilizing a 25-eV chamber voltage. Butanoic acid and butanal recovered from D_2O runs by conventional extraction techniques were also analyzed by mass spectrometry (chamber voltage employed was 25 eV). A similar analytical procedure was employed for runs with α,α-dideuteriobutanoic acid.[12]

Irradiations of Hydrocarbons. In the cases of gaseous hydrocarbons, 70 ml of the gas was bubbled into 300 ml of water purified as in the previously described cases under argon. The mixture was then irradiated for 3 hr under conditions identical with those utilized for the aldehydes and acids. The liquid hydrocarbons were added as 100-mg samples to the water–argon and irradiated similarly.

Acknowledgments. We are grateful to the Petroleum Research Fund (No. 5538-AC4) and the Research Corporation for their generous support of this work.

---

at the lower end, a disk of 500 D Mylar film serving as the sound-transparent bottom, and, at the upper end, gas inlet and outlet fixtures for control of the internal gaseous atmosphere. The vessel was fitted to an external cooling jacket by means of standard ground-glass joints which also served to maintain a reproducible distance between the surface of the transducer and the bottom of the vessel (approximately 1 cm). Sound coupling between source and vessel occurred through the water in circulation through the cooling jacket. Relative intensity measurements were made with a Macrosonics cavitation meter, Model CVM-3a. Actual intensity was estimated from the rated average output of the transducers at maximum efficiency. Infrared analyses were effected with a Perkin–Elmer Model 237B grating infrared spectrophotometer, and gc analyses accomplished with a Perkin–Elmer G-11 gas chromatograph with hot-wire detector and linear temperature programmer. A Perkin–Elmer Hitachi RMU 6 mass spectrometer was operated with a chamber voltage of 25 eV. All aldehydes and acids were purchased from Aldrich Chemical Co. All compounds were purified by distillation under an argon atmosphere with the exception of decanal and decanoic acid, which were recrystallized from hexane in a Dry Ice–acetone bath.

(11) The D_2O was 99% deuterated and was used as purchased from Stohler Isotope Chemicals.

(12) We wish to thank Dr. Terry E. Parks for his donation of the sample of α,α-dideuteriobutanoic acid which was used for these studies. A mass spectrum of this material showed it to be 95% dideuterated.

Virial Partitioning of Charge Distributions and Properties of Diatomic Hydrides

R. F. W. Bader* and P. M. Beddall

Contribution from the Department of Chemistry,
McMaster University, Hamilton, Ontario, Canada. *Received June 29, 1972*

Abstract: A spatial partitioning of the molecular charge distributions and energies of diatomic hydrides is presented. The partitioning surface is defined by the path of the gradient vector of $\rho(\mathbf{x})$, passing through the point of minimum density between the nuclei. The kinetic and potential energies of molecular fragments determined by such a surface are well defined and, in addition, satisfy the quantum mechanical virial relationship. The virial partitioning method divides a total system into subsystems, each of which is quantum mechanically self-contained. This feature is further evidenced in the observation that the constancy in the properties of a bonded fragment in different systems is reflected in the constancy of both its charge distribution *and* virial. The virial partitioning method is applied to diatomic hydrides ($HeH^+ \rightarrow HF$), neutral and charged, in their ground and excited states to yield fragment populations, kinetic and potential energies. The origin and type of binding in ground-state AH systems is described in terms of this partitioning procedure. A quantitative proposal is made, in answer to the question "are there atoms in molecules?"

In this paper we apply and illustrate an objective and fundamental partitioning procedure to properties of diatomic hydride molecules. The partitioning procedure is objective since it is unambiguously determined by the topological properties of the molecular charge distribution. It is fundamental since it yields values for the kinetic and potential energies of the fragments which are not only well defined, but satisfy the quantum-mechanical virial theorem. Thus, the *virial partitioning method* yields fragments whose average energies obey the same quantum-mechanical relationship as do the average energies of the total system.[1,2]

The fragments defined by the virial partitioning method account for one of the most important observations in chemistry: retention of the identity and properties of bonded fragments in different systems, a retention which in many instances is so close as to give rise to bond additivity schemes for the energy. The extent to which properties are additive between different systems is determined by the extent to which the charge distribu-

---

(1) R. F. W. Bader and P. M. Beddall, *J. Chem. Phys.*, **56**, 3320 (1972).

(2) R. F. W. Bader, P. M. Beddall, and J. Peslak, Jr., *ibid.*, submitted for publication.

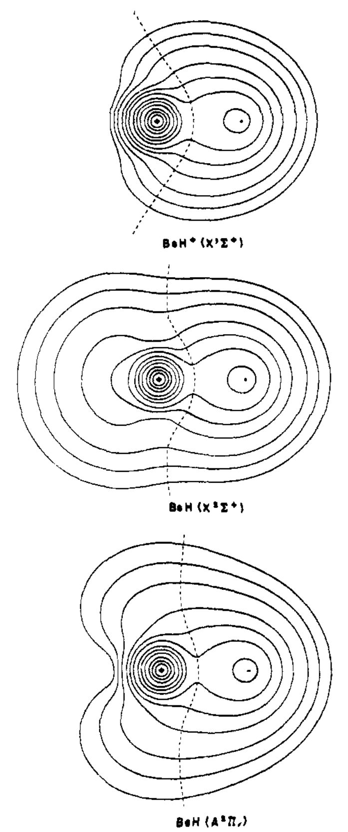

Figure 1. Contour maps of the electronic charge distribution functions for states of the BeH system illustrating the three classes of hydride molecules, BeH^+ $(X\,^1\Sigma^+)$ (class I); BeH $(X\,^2\Sigma^+)$ (class II); and BeH $(A\,^2\pi_r)$ (class III). The virial partitioning surfaces, as defined by eq 1, are indicated by dashed lines. The similarities in class characteristics between AH and AB systems are illustrated by comparing this figure with Figure 1 in ref 2 which illustrates the same classes for three states of the BeF system. The contours in this figure and Figure 2 (in au) increase in value from the outermost contour inwards in steps of 2×10^n, 4×10^n, 8×10^n. The smallest contour value is 0.002 with n increasing in steps of unity to yield a maximum contour value of 20.

tions of the corresponding fragments are unchanged by transfer between the systems.[1-3] Since the present partitioning method defines a fragment in terms of the charge distribution, it naturally accounts for the constancy of the properties of a fragment in different bonding environments in those cases where its charge distribution exhibits only small differences between two systems. Furthermore, we have presented evidence that the charge distribution of a fragment is determined by the virial of *all* the forces exerted on it.[1,2] To the extent that the *total* virial of a fragment remains unchanged between two different systems, regardless of the changes in the *individual* force contributions, the charge density and properties of the fragment remain unaltered. Thus, the method provides an explanation for the observation of bond additivity or deviations from it in terms of the external fields exerted on the fragment.

A charge distribution is partitioned by the surface $S(\mathbf{x})$ defined by the gradient vector of the charge density, $\nabla\rho(\mathbf{x})$, passing through the point of minimum density between a pair of adjacent nuclei (the point $\mathrm{d}\rho(\mathbf{x})/\mathrm{d}z = 0$, with z directed along the internuclear axis). Examples of such surfaces are shown in Figure 1 for three states of the BeH system. The new surface $S(\mathbf{x})$ follows the "path of steepest descent" through a charge distribution. It reflects the spatial properties of $\rho(\mathbf{x})$ in a more detailed manner than does the simple planar surface through the point $\mathrm{d}\rho(\mathbf{x})/\mathrm{d}z = 0$, as proposed in an earlier partitioning scheme.[4] More important, a surface $S(\mathbf{x})$ defined by $\nabla\rho(\mathbf{x})$ possesses the property that

$$\mathrm{d}\rho(\mathbf{x})/\mathrm{d}n = 0 \qquad \mathbf{x} \in S(\mathbf{x}) \tag{1}$$

where $\mathrm{d}/\mathrm{d}n$ implies differentiation with respect to the vector $\mathbf{n}$ normal to (and outwardly directed from) the surface at every point $\mathbf{x}$. It is the property of "zero flux" of $\nabla\rho(\mathbf{x})$ through $S(\mathbf{x})$ as denoted by eq 1 which makes possible the partitioning of the energy and which yields fragments which obey the virial relationship.[1,2]

Classification of Molecular Systems in Terms of $S(\mathbf{x})$

In the earlier partitioning scheme,[4] each fragment containing a given nucleus was subdivided into a bonded and a nonbonded region by a second plane drawn through the nucleus, again perpendicular to the axis. On the basis of the relative values of the bonded and nonbonded populations and of their corresponding radii, the states of diatomic molecules were divided into four classes. The same classification scheme is obtained if the shape of the surface of zero flux, $S(\mathbf{x})$, is used as the basis of the classification. Thus, AB molecules formerly placed in class I on the basis of their populations and radii possess a surface paraboloid in shape, as illustrated in Figure 1 for BeH^+ $(X\ ^1\Sigma^+)$. In systems in which the fragments possess significant net charges, the sweep of the paraboloid is such as to encompass the fragment of net positive charge: (Be) in BeH^+, (Li) in LiF.[5] Similarly, AB molecules formerly placed in class II possess a surface of zero flux with the characteristics of that shown in Figure 1 for $BeH(X\ ^2\Sigma^+)$, characteristics which are understandable in terms of the distribution of charge in class II systems. A class II system is obtained when the number of valence electrons on A (the donor) exceeds the number of vacancies on B (the acceptor) in systems containing no more than ten valence electrons. The transfer of charge from (A) to (B) is reflected in the initial paraboloid nature of $S(\mathbf{x})$ starting from the point of minimum density on the bond axis, and resembling class I systems. However, the unshared valence density in (A) is distributed in a very diffuse manner and heavily localized in the nonbonded region of (A), being repelled by net negative charge on (B). The diffuse nature of the density on (A) extends into the outer reaches of the bonded region and causes a reversal in the curvature of the outer arms of the surface $S(\mathbf{x})$. As shown later, this diffuse density distribution for (A) in class II systems possesses a relatively low kinetic energy per electron and the presence of such density coincides with the presence of chemically reactive "lone pairs" or "unshared" valence density, present, for example, in (C) of CO, (C) of CN^-, (Be) of BeF, or (B) of BF.

Class III systems exhibit the same general properties as do systems in class II and differ only in that the

---

(3) R. F. W. Bader and P. M. Beddall, *Chem. Phys. Lett.*, **8**, 29 (1971).

(4) R. F. W. Bader, P. M. Beddall, and P. E. Cade, *J. Amer. Chem. Soc.*, **93**, 3095 (1971).

(5) The symbol (A) is to be read as "the A fragment" throughout the paper.

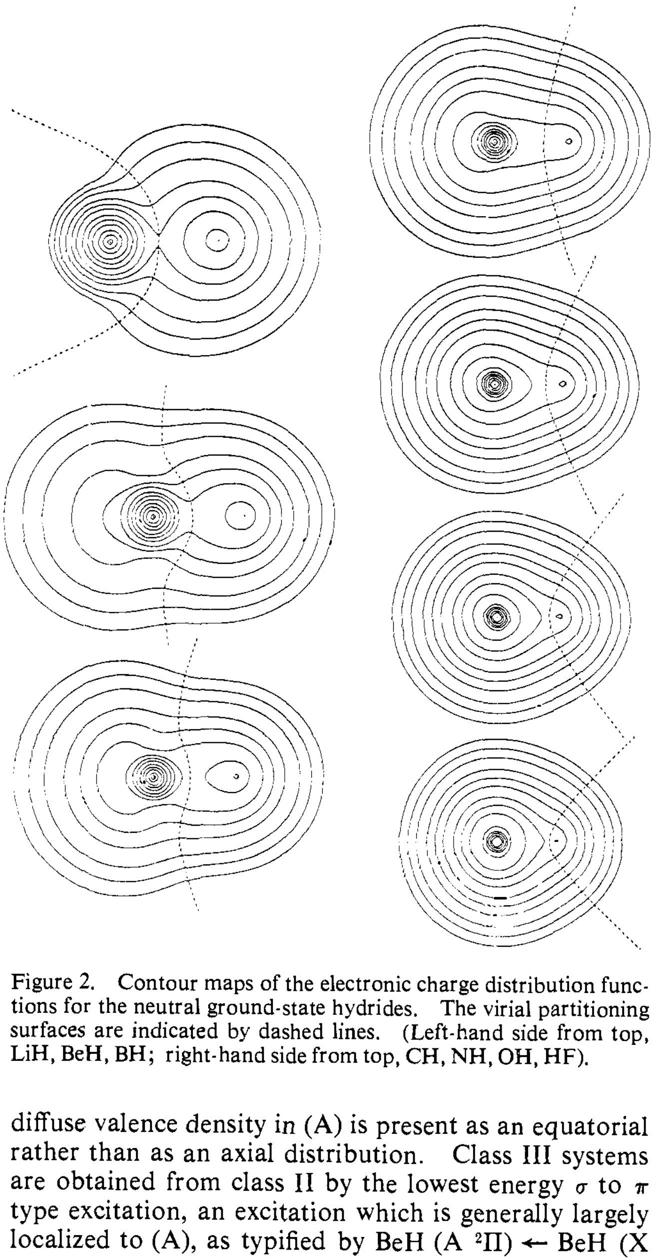

Figure 2. Contour maps of the electronic charge distribution functions for the neutral ground-state hydrides. The virial partitioning surfaces are indicated by dashed lines. (Left-hand side from top, LiH, BeH, BH; right-hand side from top, CH, NH, OH, HF).

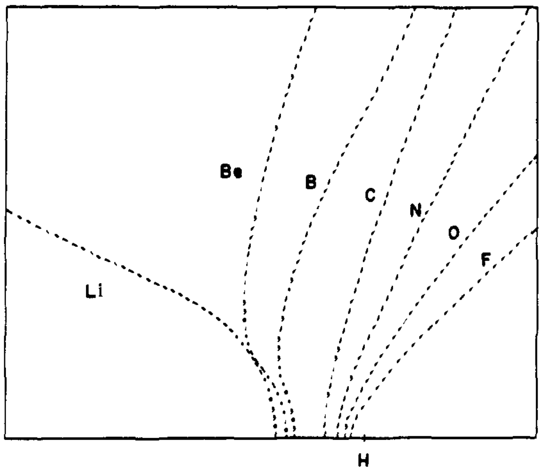

Figure 3. The partitioning surfaces for the ground-state diatomic hydrides plotted with respect to a fixed position for the proton. The distance between the intersection of $S(\mathbf{x})$ with the internuclear axis and the proton in LiH corresponds to 1.671 au.

diffuse valence density in (A) is present as an equatorial rather than as an axial distribution. Class III systems are obtained from class II by the lowest energy σ to π type excitation, an excitation which is generally largely localized to (A), as typified by BeH (A $^2\Pi$) ← BeH (X $^2\Sigma^+$), Figure 1. Similarly, removal of the diffuse nonbonded valence density on (A) in a class II system by ionization (single in BeH to yield BeH$^+$, Figure 1) yields a class I system.

Class IV systems are found for AB molecules with eleven or more valence electrons. $S(\mathbf{x})$ for such systems, *e.g.*, CF, NO, and NF, is paraboloid with a very small curvature, the surface closely approximating the limiting planar surface of homonuclear molecules. This coincides with the observation[4] that the nonbonded radii, r^n, in class IV systems correspond closely to the atomic values for both (A) and (B) (as opposed to $r_A{}^n > r_A$ for atom A and $r_B{}^n \sim r_B$ for ion B$^-$ in class II). The curvature which is present in $S(\mathbf{x})$ for class IV systems is opposite to that found in class I, the surface sloping towards (B), the fragment with a net negative charge. There are no examples of class IV systems in the diatomic hydrides.[6]

The surfaces of zero flux and their relationship to the charge distribution are illustrated in Figure 2 for the ground-state neutral diatomic hydrides. In Figure 3, the position of the proton is held fixed and the surfaces are plotted relative to this point. From the properties of the surfaces, the transfer of charge is from (A) to (H) in LiH (class I), BeH and BH (class II). The systems CH to FH are all class I. In CH, the transfer of charge is close to zero; from NH to FH an increasing amount of charge is transferred from (H) to (A) as reflected in the decreasing volume occupied by (H). Bearing in mind that the charge distribution of each fragment is a separate quantum mechanical unit in that its kinetic and potential energies satisfy a virial relationship, it is clear that almost the whole of the charge distribution in FH is governed by the potential exerted by the fluorine nucleus. It is worthwhile noting here that the charge distributions of the ionized systems FH$^+$ and NeH$^+$ are so heavily contracted towards the fluorine or neon nucleus that no minimum is found in $\rho(\mathbf{x})$ along the internuclear axis (except at infinity). Thus, FH$^+$ and NeH$^+$ are not partitionable. These systems and their properties approach, in a very real sense, those of the united atom.[7]

Virial Partitioning

In both classical and quantum mechanics the virial $\bar{V}$ of a system is defined as the average value of the scalar product of the force acting on each particle in the system with the distance of the particle from some origin

$$\bar{V} = \overline{\Sigma_i x_i(-\partial V/\partial x_i)}$$

where V is the potential (classical) or potential energy operator. The concept of the virial of a system is important because of the existence of a relationship between it and the kinetic energy $\bar{T}$, namely, the virial theorem. The theorem states that the virial of a system, in which coulombic forces are operative, is equal to minus twice the kinetic energy. Because of Euler's theorem, the virial of the electronic forces (the electron–nuclear attractions and the electron–electron repulsions) reduces to $\bar{V}_e$, the average electronic potential energy.

---

(6) A tabulation of the bonded and nonbonded charges and radii for AH systems, similar to that given previously for AB systems,[4] is available from the authors upon request.

(7) The path of the vector $\nabla\rho(\mathbf{x})$ in FH$^+$ and NeH$^+$ starting from the position of the proton at a point 1×10^{-10} au off the axis turns immediately towards the molecular axis on the nonbonded side of the proton. Thus, the volume of (H) approaches zero as the surface $S(\mathbf{x})$ collapses to a line coincident with the internuclear axis.

We shall for the moment express the virial of the nuclear forces as $\Sigma_\alpha \mathbf{R}_\alpha \cdot \mathbf{F}_\alpha$, where $\mathbf{F}_\alpha$ is the vector sum of the nuclear repulsive force on nucleus α and any external force which may be acting. $\mathbf{R}_\alpha$ is the position vector for nucleus α. The virial theorem states that

$$-2\bar{T} = \bar{V} = \bar{V}_e + \sum_\alpha \mathbf{R}\cdot\mathbf{F}_\alpha \tag{2}$$

By adding $\bar{T}$ to each side of eq 2, one obtains eq 3 where

$$-\bar{T} = \bar{E}_e + \sum_\alpha \mathbf{R}\cdot\mathbf{F}_\alpha \tag{3}$$

$\bar{E}_e$ is the average electronic energy of the system. Each of the energy quantities in eq 2 and 3 may be partitioned to yield corresponding virial relationships for the individual fragments of a total system.

The reasoning behind the proposal that the virial theorem holds for properly partitioned fragments of a total system has been given previously.[1,2] We give here only the definitions of the average values of the populations and energies for a fragment.

A. Population of a Fragment. This is obtained by integration of $\rho(\mathbf{x})$ over the volume of the fragment as defined by the surface $S(\mathbf{x})$. The population of fragment (A) is

$$\bar{N}(\mathrm{A}) = \int_\mathrm{A} \rho(\mathbf{x})\mathrm{d}\mathbf{x}$$

where the subscript A denotes an integration over the volume of (A).

B. Kinetic Energy of a Fragment. There are two possible kinetic energy distribution functions

$$K(\mathbf{x}) = -{}^1\!/_2\sum_i \lambda_i \phi_i(\mathbf{x})\nabla^2\phi_i(\mathbf{x})$$

and

$$G(\mathbf{x}) = {}^1\!/_2\sum_i \lambda_i \nabla\phi_i(\mathbf{x})\cdot\nabla\phi_i(\mathbf{x})$$

(The $\phi_i(\mathbf{x})$'s are the natural orbitals and λ_i's their occupation numbers.) Both functions when integrated over all space yield $\bar{T}$, the average kinetic energy of the system. However, the two functions will in general yield different values when integrated over an arbitrary fragment of a system since they differ in their local values. They are related by[8]

$$L(\mathbf{x}) = K(\mathbf{x}) - G(\mathbf{x}) = -{}^1\!/_4\nabla^2\rho(\mathbf{x}) \tag{4}$$

Therefore, a fragment of a system will have a well-defined, *i.e.*, unique value for its kinetic energy only if the integral of $L(\mathbf{x})\mathrm{d}\mathbf{x}$ over the volume of the fragment vanishes. The integral of $L(\mathbf{x})\mathrm{d}\mathbf{x}$ over a volume V may, by Green's theorem, be replaced by an integral over the surface bounding V

$$\int\!\!\int\!\!\int_V L(\mathbf{x})\mathrm{d}\mathbf{x} = -{}^1\!/_4\int\!\!\int_S \nabla\rho(\mathbf{x})\cdot\mathrm{d}\mathbf{S} = -{}^1\!/_4\int\!\!\int_S \frac{\mathrm{d}\rho(\mathbf{x})}{\mathrm{d}n}\mathrm{d}S$$

We have taken the requirement of a unique kinetic energy value for a fragment as being a necessary condition for any acceptable partitioning scheme. Fragments bounded by a surface $S(\mathbf{x})$ as defined by eq 1 possess this property. The average value of $L(\mathbf{x})$ vanishes for such a fragment for the same reason as it does for the total system bounded at infinity, namely, that the flux of $\nabla\rho(\mathbf{x})$ through the boundary surface is zero at all $\mathbf{x}$. The average kinetic energy of an acceptable fragment is obtained by integration of *either* $K(\mathbf{x})\mathrm{d}\mathbf{x}$ or $G(\mathbf{x})\mathrm{d}\mathbf{x}$ over the volume of the fragment[1,2]

$$\bar{T}(\mathrm{A}) \equiv \bar{G}(\mathrm{A}) = \bar{K}(\mathrm{A})$$

with $\bar{L}(\mathrm{A}) = 0$ because of the boundary condition stated in eq 1.

C. Electronic Potential Energy of a Fragment. The electronic potential energy of (A) is defined by

$$\bar{V}_e(\mathrm{A}) = -\sum_\alpha Z_\alpha \int_A (\rho(\mathbf{x})/r_\alpha)\mathrm{d}\mathbf{x} + \int_A \mathrm{d}\mathbf{x}_1 \int_V \mathrm{d}\mathbf{x}_2 \frac{\Gamma(\mathbf{x}_1,\mathbf{x}_2)}{|\mathbf{x}_1 - \mathbf{x}_2|} \tag{5}$$

or

$$\bar{V}_e(\mathrm{A}) = \bar{V}'(\mathrm{A}) + \bar{V}''(\mathrm{A})$$

$\bar{V}'(\mathrm{A})$ is the attractive energy of the charge density in (A) with all of the nuclei in the system. $\Gamma(\mathbf{x}_1,\mathbf{x}_2)$ is the two-electron probability distribution function. By integrating this function only over the volume of fragment A for one electron and over the total volume of the system V for the second electron we obtain $\bar{V}''(\mathrm{A})$, the self-repulsion of the electrons in (A) plus one-half of the total repulsion of the electrons in (A) with all the other electrons in the system.[2]

D. Nuclear Virial for a Fragment. In a diatomic system the virial of the nuclear forces reduces to

$$\sum\nolimits_\alpha \mathbf{R}_\alpha\cdot\mathbf{F}_\alpha = Z_\mathrm{A}Z_\mathrm{B}/R + R\mathrm{d}\bar{E}/\mathrm{d}R \tag{6}$$

the virial of the repulsive force between the nuclei and the virial of any external force $\mathrm{d}\bar{E}/\mathrm{d}R$ acting on the nuclei. The latter force vanishes at $R = R_e$, the equilibrium internuclear separation. In order to spatially partition the nuclear virial, it is necessary to express it in terms of the space coordinates $\mathbf{x}$. This is accomplished *via* the Hellmann–Feynman theorem which states that the nuclear force $\mathbf{F}_\alpha$ is equal and opposite to the force which the electronic charge distribution exerts on nucleus α.

$$\mathbf{F}_\alpha = -Z_\alpha\int \rho(\mathbf{x})(\mathbf{r}_\alpha/r_\alpha{}^3)\mathrm{d}\mathbf{x}$$

By integration of the expression for $\mathbf{F}_\alpha$ *over the charge distribution in just* (*A*) *one obtains the fraction of the total nuclear force balanced by the charge density in* (*A*). Thus the contribution of the nuclear virial to (A) in AB is[9]

$$\bar{V}_n(\mathrm{A}) = -\mathbf{R}_\mathrm{A}\cdot Z_\mathrm{A}\int_A \rho(\mathbf{x})(\mathbf{r}_\mathrm{A}/r_\mathrm{A}{}^3)\mathrm{d}\mathbf{x} - \mathbf{R}_\mathrm{B}\cdot Z_\mathrm{B}\int_A \rho(\mathbf{x})(\mathbf{r}_\mathrm{B}/r_\mathrm{B}{}^3)\mathrm{d}\mathbf{x}$$

or

$$\bar{V}_n(\mathrm{A}) = \mathbf{R}_\mathrm{A}\cdot\mathbf{F}_\mathrm{A}(\mathrm{A}) + \mathbf{R}_\mathrm{B}\cdot\mathbf{F}_\mathrm{B}(\mathrm{A}) \tag{7}$$

---

(8) R. F. W. Bader and H. J. T. Preston, *Int. J. Quantum Chem.*, 3, 327 (1969).

(9) In general, LCAO-MO-SCF wave functions, even those close to the Hartree–Fock limit, do not exactly satisfy the Hellman–Feynman theorem (R. Feynman, *Phys. Rev.*, **56**, 340 (1939)). Primarily because of the errors in the Hellmann–Feynman forces and hence in $\bar{V}_n$, such functions exhibit small errors in the virial relationship for the total

Table I. Virial Partitioning of Ground-State Neutral and Charged Diatomic Hydrides[a]

AH		R	$\bar{N}$(F)	$\bar{V}'$(F)	$\bar{V}''$(F)	$\bar{V}_n$(F)	$\bar{T}$(F)
LiH	$X^1\Sigma^+$	3.0150	2.0889	−17.0893	2.4124	−0.0587	7.3678
			1.9111	−3.3726	1.0759	1.0497	0.6235
BeH	$X^2\Sigma^+$	2.5380	3.1320	−33.2401	4.5426	−0.0579	14.3777
			1.8680	−4.6957	1.5146	1.6376	0.7717
BH	$X^1\Sigma^+$	2.3360	4.2461	−56.5550	8.0023	0.0948	24.2289
			1.7539	−5.7389	1.9035	2.0607	0.8874
CH	$X^2\Pi_r$	2.1240	5.9679	−90.9057	14.1670	1.4740	37.6324
			1.0321	−3.9409	1.3204	1.3753	0.6226
NH	$X^3\Sigma^-$	1.9614	7.3227	−133.4897	22.0258	2.5568	54.4536
			0.6773	−3.0683	1.0382	1.0431	0.4935
OH	$X^2\Pi_i$	1.8342	8.5849	−185.8531	32.1466	3.6766	75.0150
			0.4151	−2.2035	0.7462	0.7243	0.3665
FH	$X^1\Sigma^+$	1.7328	9.7603	−249.1576	44.8396	4.7730	99.7725
			0.2397	−1.4671	0.4938	0.4640	0.2547
HeH^+	$X^1\Sigma^+$	1.4550	1.9641	−8.1421	1.0217	1.3550	2.8827
			0.0359	−0.1316	0.0109	0.0192	0.0507
LiH^+	$X^2\Sigma^+$	3.0150	2.0369	−16.9103	2.0293	0.3098	7.2856
			0.9631	−1.9834	0.3226	0.5972	0.5318
BeH^+	$X^1\Sigma^+$	2.4790	2.2567	−31.5257	3.5158	−0.2281	14.1190
			1.7433	−4.5516	1.2442	1.8459	0.7307
BH^+	$X^2\Sigma^+$	2.2960	3.6685	−55.3131	6.7533	0.3503	24.1048
			1.3315	−4.4824	1.2533	1.8576	0.6857
CH^+	$X^1\Sigma^+$	2.1370	5.2884	−88.5758	12.0126	1.7586	37.4023
			0.7116	−2.8281	0.7820	1.0651	0.4905
NH^+	$X^2\Pi_r$	2.0480	6.5852	−129.9522	18.9373	2.7659	54.1250
			0.4148	−1.9182	0.5420	0.6940	0.3411
OH^+	$X^3\Sigma^-$	1.9440	7.7661	−181.2054	28.0222	3.7160	74.7336
			0.2339	−1.2572	0.3587	0.4359	0.2313
CH^-	$X^3\Sigma^-$	2.0860	6.7332	−92.7187	16.1070	1.3368	37.6375
			1.2668	−4.6857	1.7944	1.4929	0.6992
NH^-	$X^2\Pi_i$	1.9230	8.1644	−135.9655	24.7231	2.4695	54.3865
			0.8356	−3.6717	1.4063	1.1458	0.5597
OH^-	$X^1\Sigma^+$	1.7810	9.4328	−189.2369	35.6944	3.5884	74.9770
			0.5672	−2.9079	1.1149	0.8948	0.4491

[a] (F) denotes either an (A) or (H) fragment. The properties of (A) are listed above those for (H) in each system. Wave functions for ground-state hydrides are from Cade and Huo,[17] OH^-, from P. E. Cade, *J. Chem. Phys.*, **47**, 2390 (1967), remaining functions from P. E. Cade by private communication.

Table II. Virial Partitioning of Excited-State Diatomic Hydrides[a]

AH		R	$\bar{N}$(F)	$\bar{V}'$(F)	$\bar{V}''$(F)	$\bar{V}_n$(F)	$\bar{T}$(F)
BeH	$A^2\Pi_r$	2.5380	3.0725	−33.0039	4.4629	−0.0706	14.3058
			1.9275	−4.6565	1.5390	1.6651	0.7262
BH^+	$A^2\Pi_r$	2.2960	3.8449	−55.6777	6.9420	0.5548	24.0904
			1.1551	−3.9336	1.1257	1.6250	0.5915
CH	$a^4\Sigma^+$	2.0836	6.2242	−91.8503	14.5852	1.8413	37.7119
			0.7758	−3.0506	0.9949	1.0658	0.4950
CH	$A^2\Delta$	2.0836	6.2395	−91.7801	14.5802	1.8619	37.6690
			0.7605	−2.9892	0.9716	1.0404	0.4886
CH	$B^2\Sigma^-$	2.2414	6.2955	−91.7556	14.5361	1.8235	37.6981
			0.7045	−2.6279	0.8752	0.8746	0.4390
CH	$C^2\Sigma^+$	2.1037	6.2592	−91.6935	14.5661	1.8774	37.6250
			0.7408	−2.8899	0.9366	1.0027	0.4753
NH	$A^3\Pi$	1.9600	7.5792	−134.3625	22.4844	2.9450	54.4665
			0.4208	−1.9637	0.6260	0.6559	0.3410
NH	$c^1\Pi$	2.1263	7.5313	−133.6431	22.2068	2.6446	54.3959
			0.4687	−2.0301	0.6750	0.6624	0.3464
NH	$a^1\Delta$	1.9729	7.3395	−133.3733	22.0192	2.5773	54.3884
			0.6605	−2.9831	1.0070	1.0103	0.4829
OH	$A^2\Sigma^+$	1.9120	8.7582	−186.2850	32.4570	3.7950	75.0165
			0.2418	−1.2826	0.4124	0.4062	0.2320
OH^+	$A^1\Delta$	1.9440	7.7766	−181.0963	28.0410	3.7273	74.6640
			0.2234	−1.1994	0.3395	0.4132	0.2234

[a] (F) denotes either an (A) or (H) fragment. The properties of (A) are listed above those for (H) in each system. Wave functions for excited states of CH and NH from W. M. Huo, *J. Chem. Phys.*, 49, 1482 (1968); remaining functions from P. E. Cade by private communication.

Because of the presence of the position vectors $\mathbf{R}_\alpha$ in eq 7, the nuclear contribution to the virial is origin dependent. We have previously shown, however, that the position of the origin defining the values of $\mathbf{R}_\alpha$ is not arbitrary but is fixed by a property of the system,[2] and that in general, it is found to be close to the bond midpoint.

---

molecule.[1,2] For example, Δ ($= 2\bar{T} + \bar{V}$) = 0.0141 au in LiH and 0.0572 au in HF. (A tabulation of Δ values is given in ref 2.) For the purpose of discussing energy changes, the small errors in $\bar{V}_n$ are ignored and the values of $\bar{V}_n$(A) and $\bar{V}_n$(H) given in Tables I and II are such that they satisfy the fragment virial relationship exactly.

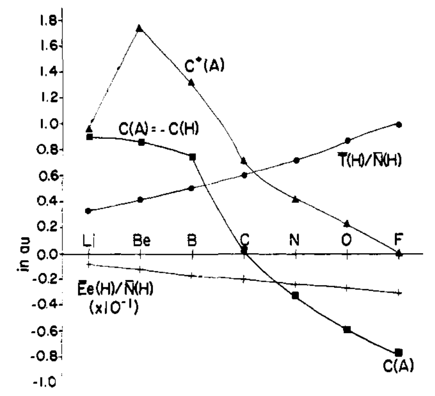

Figure 4. The variation with nuclear charge of C(A), the net charge on (A), and the average kinetic and electronic energies per electron for (H) in neutral ground state AH, and C^+(A), the net charge on (A) in ground state AH$^+$.

Virial Partitioning of Diatomic Hydrides

Partitioning of Total Molecular Properties. The results of the virial partitioning as applied to diatomic hydrides, both neutral and charged, in their ground and excited states are given in Tables I and II. The variation in the populations $\bar{N}$(A) and $\bar{N}$(H) through the series of neutral hydrides shows a change in the gross features of the charge distributions from a nearly ionic system in LiH to a homopolar system in CH, ending in a very polar system with HF, a similar but more quantitative statement of the conclusion obtained from an earlier study of the charge distributions.[10] Figure 4 shows a plot of the net charge on (A), $C(\mathrm{A}) = Z_\mathrm{A} - \bar{N}(\mathrm{A}) = -C(\mathrm{H})$, *vs.* Z_A. There is a sharp discontinuity in this plot between BH and CH. The value of $\bar{N}$(H) and hence C(A) changes by only 0.04 electron between LiH (class I) and BeH (class II) as the additional valence electron in BeH is almost totally localized in the nonbonded region of (Be). This is the characteristic feature of class II systems and the same observation applies to BH where the population on the proton is only 0.16 electron less than in LiH. The values of the nonbonded charges on (A) in LiH, BeH, and BH, 1.06, 1.96, and 2.75, respectively, indicate the extent to which the unshared valence electrons are localized in the nonbonded regions of (Be) and (B), with the result that the net charges on (A) and (H) change very little. In CH there is a large reduction in $\bar{N}$(H) and the disparity between the bonded and nonbonded populations on (A) drops in value, reflecting a very even sharing of the valence charge density over both fragments. In the remaining systems the charge distribution is increasingly localized in (A).

Also illustrated in Figure 4 is C^+(A), the net charge on (A) in AH$^+$. The extent of loss of electronic charge from (A) on ionization of AH, $C^+(\mathrm{A}) - C(\mathrm{A})$, is nearly zero for (Li) and ~0.9 for (Be), a reflection of the presence of loosely bound unshared charge density in (Be). The values of $\bar{N}$(H) in CH$^+$, NH$^+$, and OH$^+$ are very similar to those for NH, OH, and HF, respectively. Since these molecular ions dissociate to A$^+$ + H, the pairs C$^+$ and N, N$^+$ and O, O$^+$ and F have nearly equal electron withdrawing abilities.[11]

The kinetic and electronic potential energies of (A) exhibit a continuous increase and decrease, respectively, through the series. These values reflect the increasing nuclear charge and are dominated by the contributions from the core electrons. The energy components of (H), on the other hand, are free of this complication. All of the component energies of (H) exhibit a discontinuity between BH and CH, paralleling the discontinuity observed in $\bar{N}$(H). Their absolute values reach a maximum at BH. The existence of a discontinuity in the type of bonding in the second-row hydrides has been predicted by Fajans,[12] who placed it between BH and CH, and by Blinder,[13] who maintained that the discontinity should occur between BeH and BH. The discontinuity in the variation of (H) energies *vs.* Z_A disappears when one plots the energy per electron. This is illustrated in Figure 4 which shows both the kinetic and total electronic energies per electron ($\bar{T}(\mathrm{H})/\bar{N}(\mathrm{H})$ and $\bar{E}_\mathrm{e}(\mathrm{H})/(\bar{N}(\mathrm{H}))$) for (H) in the series of neutral hydrides. The magnitudes of both quantities show a monotonic change with Z_A, nearly linear for $\bar{E}_\mathrm{e}(\mathrm{H})/\bar{N}(\mathrm{H})$. The increase in the kinetic energy per electron of (H) is a result of the increasing contraction of the charge density in this fragment as Z_A is increased (see Figure 2). It is a consequence of Heisenberg's uncertainty relationship that the more confined a particle, the greater is its kinetic energy. In terms of the charge distribution, one finds that a diffuse distribution yields a low kinetic energy ((H) in LiH being the most diffuse in this series) while a contracted distribution yields a high kinetic energy (the charge density of (H) in HF being the most contracted).

The nuclear virial for a fragment deserves more detailed comment as it determines the fraction of the total nuclear repulsive potential experienced by each fragment. In other words, eq 7 states that the nuclear virial for a fragment is equal to the sum of the virials of the forces exerted on each of the nuclei in the system by the charge density in the fragment. Since the forces are readily related to the nature of the charge distribution, the partitioning of the nuclear potential between the fragments of a system is easily visualized. As we have shown before,[10,14] the direction and magnitude of the forces exerted on the nuclei by the charge density in various spatial regions is characteristic of the binding in the system, whether it is an ionic, covalent or a polar system. LiH is characterized by a transfer of nearly one electronic charge from (Li) to (H) and in this case each fragment distribution exerts a force on the nucleus

---

[10] R. F. W. Bader, I. Keaveny, and P. E. Cade, *J. Chem. Phys.*, 47, 3381 (1967).

[11] The (A) populations in AH may be used to define a bonding electron affinity (an electronegativity) which in turn may be used to predict fragment populations in other systems. Define the bonding affinity relative to hydrogen as $X(\mathrm{A}) = 1 - \bar{N}(\mathrm{H})_\mathrm{AH}$, where $\bar{N}(\mathrm{H})_\mathrm{AH}$ is the (H) population in AH. $X(\mathrm{A}) \gtrless 0$ implies a bonding electron affinity for A greater or smaller than that of H. The population of (A) in AB is then $\bar{N}(\mathrm{A})_\mathrm{AB} = [\bar{N}(\mathrm{A})_\mathrm{a} - (X(\mathrm{B}) - X(\mathrm{A}))v]$ where v equals the number of valence electrons on A or vacancies on B, whichever is the lesser of the two. Predicted and actual fragment populations for (A) are: NF, 6.56 (6.56); NO, 6.46 (6.50); CF, 5.21 (5.22); CO, 4.78 (4.65); CN, 4.94 (4.88); LiC, 2.12 (2.12). With the added stipulation that the charge transferred per valency, $|X(\mathrm{B}) - X(\mathrm{A})|$, cannot exceed v, then all diatomic fluoride populations are predicted to within a maximum error of 0.08 electron, $\bar{N}$ (Li in LiN being 2.08 electrons). This simple rule is in serious error only for oxides, nitrides, and carbides of Be and B for which the degree of charge transfer is overestimated, *e.g.*, BO, 3.00 (3.45).

[12] K. Fajans, *J. Chem. Phys.*, 40, 1773 (1964); **41**, 4005 (1964); **43**, 2159 (1965).

[13] S. M. Blinder, *ibid.*, 41, 4004 (1964).

[14] R. F. W. Bader, W. H. Henneker, and P. E. Cade, *ibid.*, **46**, 3341 (1967).

external to it which approximates that obtained from a spherical charge distribution with the same number of electrons.[2] Since $(\bar{N}(\mathrm{H}) - Z_{\mathrm{H}}) \sim 1$, the Li nucleus experiences a net attractive or *binding* force from (H). To balance this, the charge density in (Li) is polarized away from (H) and $F_{\mathrm{Li}}(\mathrm{Li})$ is repulsive or *antibinding*. The proton, on the other hand, experiences a net repulsive field from (Li) since $(N(\mathrm{Li}) - Z_{\mathrm{Li}}) \sim -1$. The charge density of (H) is, therefore, polarized towards (Li) and exerts a binding force on the proton. These polarizations are characteristic of an ionic system in class I; the charge distributions of both fragments are polarized in a direction counter to the direction of charge transfer.[10,14] The nuclear virial for (Li) in LiH is

$$\bar{V}_n(\mathrm{Li}) = \mathbf{R}_{\mathrm{Li}}\cdot\mathbf{F}_{\mathrm{Li}}(\mathrm{Li}) + \mathbf{R}_{\mathrm{H}}\cdot\mathbf{F}_{\mathrm{H}}(\mathrm{Li})$$

where $\mathbf{R}_{\mathrm{Li}}$ and $\mathbf{R}_{\mathrm{H}}$ are measured from the origin which, in this case, is shifted slightly from $R/2$ towards the proton.[2] A binding force gives a positive contribution to $\bar{V}_n$; an antibinding force gives a negative contribution. In the present case, $\mathbf{F}_{\mathrm{Li}}(\mathrm{Li})$ is antibinding and $\mathbf{F}_{\mathrm{H}}(\mathrm{Li})$ is binding and their corresponding virials are thus of opposite sign. The net result is that $\bar{V}_n(\mathrm{Li})$ is small, and, in fact, slightly negative. For (H), both $\mathbf{F}_{\mathrm{H}}(\mathrm{H})$ and $\mathbf{F}_{\mathrm{Li}}(\mathrm{H})$ are binding, their virials add and $\bar{V}_n(\mathrm{H})$ is slightly greater than the total value of $\bar{V}_n$. In just those cases where $\bar{V}_n(\mathrm{A})$ is predicted to be negative, LiH, BeH, BeH$^+$, and only these cases, one finds $|2\bar{T}(\mathrm{A})| > |\bar{V}_e(\mathrm{A})|$. Since $-2\bar{T}(\mathrm{A}) = \bar{V}_e(\mathrm{A}) + \bar{V}_n(\mathrm{A})$ by the virial theorem, $\bar{V}_n(\mathrm{A})$ must be negative if the virial theorem is to be satisfied for these fragments. The very unequal partitioning of $\bar{V}_n$ in these cases is a direct result of the large counter-polarization of the charge distribution in the (A) fragment and is characteristic of ionic AH and AH$^+$ in class I and of AH and AH$^+$ in class II. In class II systems, the value of $\mathbf{F}_{\mathrm{A}}(\mathrm{A})$ is again antibinding (and large in magnitude) because of the localization of the unshared *valence* density in the nonbonded region of (A).

The charge distributions of CH and the polar systems (class I with charge transfer from H → A) are characterized by having both fragment distributions polarized into the bond. Thus, all four force contributions, $\mathbf{F}_{\mathrm{A}}(\mathrm{A})$, $\mathbf{F}_{\mathrm{H}}(\mathrm{A})$, $\mathbf{F}_{\mathrm{H}}(\mathrm{H})$ and $\mathbf{F}_{\mathrm{A}}(\mathrm{H})$, are binding and their virials add for each fragment. The homopolar nature of CH is reflected in an almost equal sharing of $\bar{V}_n$ between the two fragments: $\bar{V}_n(\mathrm{C}) = 1.4740$ au; and $\bar{V}_n(\mathrm{H}) = 1.3753$ au. In NH → HF, the (A) assumes an increasing share of $\bar{V}_n$ as a result of the decreasing population of the (H) fragment.

The fragment values listed in Tables I and II allow for a quantitative partitioning of the energy changes associated with any physical process. In addition, the energy changes may be directly related to the changes in the distribution of charge within the system. This is illustrated through the virial partitioning of the binding energies and ionization energies of some diatomic hydrides.

Partitioning of Binding Energies in AH. Application of the virial theorem to the energy changes associated with bond formation yields eq 8 where Δ denotes the

$$-2\Delta\bar{T} = \Delta\bar{V}' + \Delta\bar{V}'' + \Delta\bar{V}_n \qquad (8)$$

difference between the molecular and the sum of the corresponding atomic quantities. For example

$$\Delta\bar{T} = \bar{T}(\mathrm{AH}) - \bar{T}_{\mathrm{a}}(\mathrm{A}) = \bar{T}_{\mathrm{a}}(\mathrm{H})$$

The subscript "a" denotes the atomic state for (A) or (H). Since $\bar{V}_n$ is zero for the separated atoms

$$\Delta\bar{V}_n = \bar{V}_n(\mathrm{AH}) = Z_{\mathrm{A}}Z_{\mathrm{B}}/R + R\mathrm{d}\bar{E}/\mathrm{d}R \qquad (9)$$

The virial of the external forces $R\mathrm{d}E/\mathrm{d}R$ vanishes when R equals the equilibrium value R_{e} and $\bar{V}_n(\mathrm{AH})$ then equals simply the virial of the nuclear repulsion forces. In this situation, $-\Delta\bar{T}$ is equal to the *total* energy change ΔE in the system, the binding energy of AH.

$$-\Delta\bar{T} = \Delta\bar{E}_{\mathrm{e}} + \bar{V}_n = \Delta\bar{E} \qquad (10)$$

In the process of bond formation, $\Delta\bar{V}'' > 0$ and $\Delta\bar{V}_n > 0$ and the total energy of the system can be lowered only if $\Delta\bar{V}' < 0$. Thus, a molecule is stable relative to the separated atoms only if the redistribution of charge density accompanying its formation results in a decrease in the nuclear-electron potential energy and then only if the magnitude of this decrease is in excess of the increases in the electron–electron and nuclear repulsive energies. The extent by which the attractive interactions exceed the repulsive ones is, according to eq 8, given by $-2\Delta\bar{T}$. Thus, one has the well-known result that the kinetic energy of the total system must increase if the molecule is to be stable relative to the separated atoms.[15]

Since the present partitioning procedure yields fragments which separately obey the virial relationship, we may determine the contribution of each fragment to the total binding energy of the system. Application of the virial partitioning to the molecular terms in eq 8 and 10 yields, for either fragment

$$-2\Delta\bar{T}(\mathrm{A}) = \Delta\bar{V}'(\mathrm{A}) + \Delta\bar{V}''(\mathrm{A}) + \Delta\bar{V}_n(\mathrm{A}) \qquad (11)$$

and

$$-\Delta\bar{T}(\mathrm{A}) = \Delta\bar{E}_{\mathrm{e}}(\mathrm{A}) + \bar{V}_n(\mathrm{A}) = \Delta\bar{E}(\mathrm{A}) \qquad (12)$$

where

$$\Delta\bar{T}(\mathrm{A}) = \bar{T}(\mathrm{A}) - \bar{T}_{\mathrm{a}}(\mathrm{A})$$

with corresponding definitions for the other quantities. We have also assumed in eq 12 that $R\mathrm{d}\bar{E}/\mathrm{d}R = 0$.[16] While the kinetic energy of the total system must increase if the molecule is to be stable relative to the separated atoms, the changes in the average values of the fragment kinetic energies may be positive or negative. In what follows, the sign of $\Delta\bar{T}(\mathrm{A})$ will be used to determine, *via* eq 11, the increase or decrease in the potential interactions of (A) on bonding and, *via* eq 12, the increase or decrease in its stability relative to the atom A.

The changes in the fragment energies on bond formation are listed in Table III. Since the rationalized Hartree–Fock binding energies do not account for the changes in the correlation energy, the following discus-

---

(15) For relatively large internuclear separations (in the attractive range of a potential curve) the virial of the attractive force $R\mathrm{d}E/\mathrm{d}R$ is positive and may exceed the decrease in E for the system. In this case T for the system can be less than the sum of the separated atom kinetic energies. This behavior is found for example in $\mathrm{H}_2(\mathrm{X}^1\Sigma^+)$.[8] It cannot occur in the neighborhood of R_{e} where $R\mathrm{d}E/\mathrm{d}R$ is small or zero.

(16) The wave functions for the neutral ground-state hydrides are calculated for their experimental equilibrium R_{e} values. Hence, the calculated net nuclear forces are very small and $R\mathrm{d}E/\mathrm{d}R$ is of the order of magnitude or smaller than the errors in the total virial relationship.

Table III. Changes in Fragment Energies on Bond Formation for Ground-State Diatomic Hydrides[a]

AH(X)	ΔT(A)	$\Delta V'$(A)	$\Delta V''$(A)	ΔE_e(A)	ΔT(H)	$\Delta V'$(H)	$\Delta V''$(H)	ΔE_e(H)
LiH	−0.0649	+0.05713	+0.13141	+0.1236	+0.1235	−2.3245	+1.0278	−1.1732
BeH	−0.1953	+0.39539	+0.05302	+0.2531	+0.2717	−3.6956	+1.5146	−1.9093
BH	−0.3005	+0.34243	+0.16343	+0.2058	+0.3874	−4.7393	+1.9038	−2.4481
CH	−0.0560	−2.76986	+1.40806	−1.4180	+0.1225	−2.9411	+1.3209	−1.4977
NH	+0.0520	−5.13769	+2.47622	−2.6088	−0.0065	−2.0691	+1.0390	−1.0366
OH	+0.2055	−7.77876	+3.69076	−3.8821	−0.1338	−1.2040	+0.7473	−0.5905
FH	+0.3639	−10.49188	+4.99162	−5.1370	−0.2453	−0.4684	+0.4951	−0.2186

[a] The values are in each case the fragment value minus the corresponding Hartree–Fock ground-state atomic value.

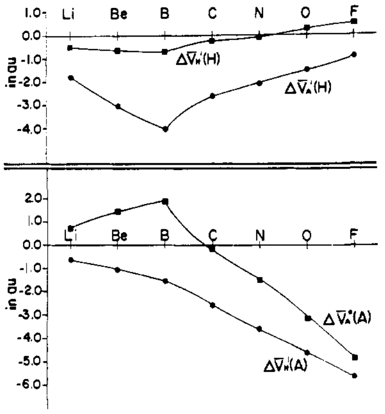

Figure 5. Changes in the electron–nuclear attractive energies on formation of ground-state AH.

sion is limited to the trends in the quantities which contribute to the binding energies in the AH sequence.[17]

In the three systems characterized by a large transfer of charge from A to H, LiH, BeH, and BH, one finds $\Delta\bar{T}$(A) < 0 and $\Delta\bar{T}$(H) > 0. Thus, in these systems it is the transfer of charge density to and its distribution in (H) which is responsible for the decrease in energy on bond formation, (A) being destabilized relative to the isolated A atoms. The destabilization of (A) as measured by the decrease in their average kinetic energies is a result of the substantial transfer of valence charge density to a region of relatively high potential, the proton in (H).

The observations are to be contrasted with those for the hydrides NH, OH, and HF which are characterized by an increasing degree of charge transfer from H to A. In these molecules, $\Delta\bar{T}$(A) > 0 and $\Delta\bar{T}$(H) < 0 and the binding in these systems results from an increase in the stabilization of (A). Since the transfer of charge in these systems is from a region of high potential (the proton) to a region of relatively low potential (the A nucleus) one anticipates a greater degree of binding in these polar compounds than is found in the species LiH, BeH, and BH. The CH system, which is intermediate in that the charge transfer between the fragments is nearly zero, is also, as discussed below, intermediate in the nature of the energy changes leading to chemical binding.

The dominant energy change in bond formation, and the only quantity for which a change in value can lead to chemical stability is $\Delta\bar{V}'$, the electron–nuclear attractive energy. The changes in this quantity for each fragment parallel closely one's intuitive knowledge of the chemistry of the second-row elements and their relative electronegativities. On the basis of the values of $\Delta\bar{V}'$ for the individual fragments an understanding of the binding can be obtained.

The value of $\bar{V}'$(X) for a fragment X in XY is equal to $\bar{V}_X'$(X), the attraction of nucleus X for the charge density in (X), and $\bar{V}_Y'$(X), the attraction of the external nucleus (or nuclei) for the same charge density. Similarly $\Delta\bar{V}'$(X) may be equated to the sum of $\Delta\bar{V}_X'$(X) $=$ $\bar{V}_X'$(X) $-$ $\bar{V}_a'$(X) and $\Delta\bar{V}_Y'$(X) $\equiv$ $\bar{V}_Y'$(X). That is, $\Delta\bar{V}_X'$(X) measures the change in the attractive interaction of nucleus X with its own charge density on changing from the atom X to the fragment (X) in the molecule while $\bar{V}_Y'$(X) measures the new interaction of the charge density in (X) with the nucleus (or nuclei) in the fragment to which (X) is bonded. These contributions to $\Delta\bar{V}'$(A) and $\Delta\bar{V}'$(H) for the first-row diatomic hydrides are shown plotted in Figure 5.

The loss of nearly a single valence electron from (A) in LiH, BeH, and BH increases the value $\bar{V}_A'$(A) relative to the atomic value $\bar{V}_a'$(A). The attractive interaction of the charge density remaining in (A) with the proton, $\bar{V}_H'$(A), is in each case less than the increase in $\bar{V}_A'$(A) over the atomic value. Thus, $\Delta\bar{V}'$(A) is positive and destabilizing in all three cases and $\Delta\bar{T}$(A) must necessarily be less than zero for these fragments.

The charge density transferred to the proton in the same three systems results in a decrease in $\bar{V}'$(H) relative to the atomic value and it is this decrease which is responsible for the small net binding found in these molecules. The attractive interaction of the proton with the charge density in (H) does increase slightly on binding ($\Delta\bar{V}_H'$(H) < 0) by a nearly constant amount for all three systems. However, the principle cause of the decrease in $\bar{V}'$(H) arises from the attraction of nucleus A for the charge density in (H), an effect which increases markedly as the nuclear charge of A increases. The increase in the strength of the AH bond from LiH to BH may be directly related to the increase in the attractive interaction of the A nucleus with the charge density of (H) as the nuclear charge of A increases. The large negative values of $\bar{V}_A'$(H) are remarkable in that they indicate that the attractive interaction of the A nucleus with the valence charge density transferred to (H) is larger than when the same density was centered on A in the atomic state. (That is, in each case $|\Delta\bar{V}_A'(A)| < {}^1/_2|\Delta\bar{V}_A'(H)|$ and less than one electron is transferred from A → H in each case.)

Both fragments in the polar systems undergo an increase in stability in terms of the electron–nuclear and electron–electron interactions relative to the separated atoms. Because of the loss of charge density from the

---

[17] P. E. Cade and W. M. Huo [*J. Chem. Phys.*, 47, 614 (1967)] give a detailed discussion of the correlation energies for the ground-state AH series. The calculated and experimental values of D_e (the latter in parentheses) in eV are: LiH, 1.48 (2.52); BeH, 2.15 (2.6); BH, 2.78 (3.54); CH, 2.47 (3.65); NH, 2.10 (3.9); OH, 3.03 (4.63); HF, 4.38 (6.11).

proton, $\Delta\bar{V}_H'(H) > 0$. However, $\bar{V}_A'(H)$, the attractive interaction of the F, O, or N nucleus for the remaining charge density in (H), is large and negative and $\Delta\bar{V}'(H)$ is overall negative, but increasingly less so from NH to HF. In the polar molecules the major contribution to the binding comes from the large decrease in $\bar{V}'(A)$. The value of $\Delta\bar{V}_A'(A) < 0$ and becomes increasingly more so from NH → FH as a result of the increasing nuclear charge of A and the accompanying increase in the degree of charge transfer from H → A. Of even larger magnitude, however, is $\bar{V}_H'(A)$, the attractive interaction of the proton with the charge density in (A). The binding in the polar hydrides arises primarily from the very large attractive interactions of both the A and H nuclei for the charge density in (A). It is interesting to compare the value of -10.5 au for $\Delta\bar{V}'(F)$ obtained from the transfer of 0.76 electron from H to F in HF with the value of -4.7 au for $\Delta\bar{V}'(H)$ obtained in BH for the transfer of 0.75 electron from B to H.

The CH system which is intermediate between LiH, BeH, BH, and the polar molecules in that the charge transfer between the fragments is nearly zero, is also intermediate in the nature of the energy changes leading to binding. In this case $\Delta\bar{T}(C) < 0$ and $\Delta\bar{T}(H) > 0$ as in the ionic cases, but $\Delta\bar{V}'$ and $\Delta\bar{E}_e$ are less than zero for both fragments as in the polar molecules. The redistribution of charge density in each fragment leads to a small increase in the attractive interaction of each nucleus with its own fragment density over the atomic values. The major contribution to $\Delta\bar{V}'$ for both fragments, however, is a result of the attractive interaction between each fragment density and the nucleus external to it, $\Delta\bar{V}_H'(C) = -2.6$ au and $\Delta\bar{V}_C'(H) = -2.7$ au. Thus, in LiH, BeH, and BH, characterized by a large transfer of charge from A → H, the binding is primarily the result of the attractive interaction of nucleus A with the charge density of (H); in the polar systems NH, OH, and HF with increasing charge transfer H → A, it is the result of the attractive interactions of both the H and A nuclei with the charge density in (A); in CH, with approximately zero charge transfer, the binding results equally from the attraction of the C nucleus for the density of (H) and of the proton for the density of (C). The values of $\Delta\bar{V}'$, $\Delta\bar{V}''$, and $\Delta\bar{V}_n$ are nearly identical for both the (C) and (H) fragments in the formation of CH. Thus the binding in CH is best described as homopolar as the energy changes closely approximate those for a homonuclear diatomic system with an equal sharing of the total charge distribution. It is remarkable that in spite of the great dissimilarity in the total populations of the two fragments, the changes in all of the potential contributions for both (C) and (H) in the formation of CH are so similar.

Reference to Tables I and III shows that aside from (Li), (Be), and (B), the share of the total nuclear repulsion for both the (A) and (H) fragments is very similar to the increase in the average electron–electron repulsive interactions for each fragment. For example, in NH, $\Delta\bar{V}''(N) = 2.48$ au, $\Delta\bar{V}_n(N) = 2.56$ au, $\Delta\bar{V}''(H) = 1.04$ au, and $\Delta\bar{V}_n(H) = 1.04$ au. In (N), (O), and (F) for which $\Delta\bar{T}(A) > 0$, the sum of $\Delta\bar{V}''(A)$ and $\Delta\bar{V}_n(A)$ is a few per cent less than the magnitude of $\Delta\bar{V}'(A)$. Thus, the larger the magnitude of the decrease found in $\Delta\bar{V}'(A)$, the larger is the net binding in the system.

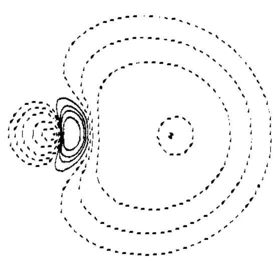

$\Delta\rho$ $LiH^+(X^2\Sigma^+) - LiH(X^1\Sigma^+)$

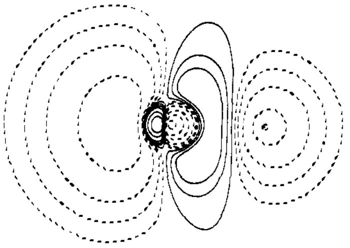

$\Delta\rho$ $BeH^+(X^1\Sigma^+) - BeH(X^2\Sigma^+)$

Figure 6. Difference maps ($\rho_{AH^+}(\mathbf{x}) - \rho_{AH}(\mathbf{x})$) showing the changes in the molecular charge distributions for vertical ionizations of ground-state LiH and BeH to ground-state molecular-ions. The first solid contour adjacent to a dashed one is a zero line; the contours increase (solid) and decrease (dashed) from this zero line in steps of $\pm 2 \times 10^n$, $\pm 4 \times 10^n$, $\pm 8 \times 10^n$ beginning with $n = -3$ and increasing in steps of unity to a maximum contour value of 20 au. The proton is on the right-hand side. Note the opposite directions of the core polarizations in (Li) and (Be).

Partitioning of Ionization Energies. The principal features of the change in the distribution of charge caused by the vertical ionization of LiH are illustrated in Figure 6: a *removal* of charge density which is confined almost totally to (H), $\Delta\bar{N}(H) = -0.95$, and a *polarization* of the charge density in (Li) towards the proton. Because the loss of charge from (Li) is small, $\bar{V}'(Li)$ increases by only a small amount (0.179 au). The self-repulsion of the electrons in (Li) remains nearly unchanged on ionization, but the contribution to $\bar{V}''(Li)$ arising from the repulsion of the electrons in (Li) by those in (H) is significantly lowered because of the reduction in $\bar{N}(H)$, and overall $\Delta\bar{V}''(Li)$ decreases by 0.383 au. This decrease is almost totally compensated for by an increase of 0.369 au in $\Delta\bar{V}_n(Li)$, an increase which is directly related to a reduction in the polarization of (Li). The loss of nearly one electronic charge from (H) reduces the net negative (attractive) field exerted on the Li nucleus. Thus, the counterpolarization of the (Li) fragment and its associated antibinding force $F_{Li}(Li)$, present in the neutral molecule to achieve electrostatic equilibrium, are greatly reduced in the molecular-ion. The reduction in the counterpolarization of (Li) as evidenced in Figure 6 reduces the antibinding force exerted on the Li nucleus by (Li) and the negative contribution to the nuclear virial of (Li) is correspondingly reduced. The value of the binding force exerted on (Li) by the proton remains nearly unchanged as $\bar{N}(Li)$ remains nearly constant. Thus, the contribution of the nuclear virial to (Li) increases on ionization and the total change in its virial is minimized.

It is of interest to contrast the changes for (Li) on ionization of LiH with those for (Be) on ionization of BeH. The charge transfer from A to H is only slightly less in BeH than in LiH. Thus, the charge distribution of (Be) must exert a large antibinding force on the Be nucleus (as does (Li) on the Li nucleus in LiH) to balance the net attractive field exerted by (H). Unlike LiH, the population of (H) decreases only slightly in the ionization of BeH. Hence, the (Be) density must exert an antibinding force on the Be nucleus in the molecular-ion, as well as in the neutral molecule. In neutral BeH, the antibinding force is exerted primarily by the diffuse distribution of valence density localized in the nonbonded region of (Be). This diffuse distribution is lost on ionization and hence in the molecular-ion, the antibinding force must be obtained by a polarization of the (Be) core density.

These features are very evident in Figure 6 giving a density difference map between BeH^+ and BeH. There is a large region of charge removal from (Be), primarily from its nonbonded region. There is a polarization of the remaining core density of (Be) away from the proton, just the reverse of the polarization found in the ionization of LiH. There is a region of charge increase and of charge decrease in the (H) fragment which integrates to a small net decrease in $\bar{N}$(H) and represents primarily a polarization of the (H) density towards (Be). This latter polarization is understandable in the light of the increase in the positive attractive field exerted by (Be) on (H) because of the loss of approximately nine-tenths of an electronic charge from (Be).

Conclusion and Discussion

We have avoided using the term atomic in the labeling of the fragments and their properties since in general the charge distributions of the free atoms are greatly changed when combined in the molecular state. If we reserve the name atom for the symmetrical distribution of charge bound to a single nucleus in field-free space (an isolated, mononuclear fragment), then by definition the term atom will never be applicable to a fragment in a molecular system. But the question of real interest, regardless of definitions, is the extent to which a given fragment in a molecule deviates in properties and structure from its parent atomic (or ionic) state. Changes in populations and energies from the atomic values are of interest but do not serve the purpose of indicating how the total energy is structured relative to the atomic state. More important is the manner in which the balance between the various contributing field is attained in the molecule compared to the atom.

In answer to the question "are there atoms in molecules," we propose that one compare how nearly the internal electronic fields of a fragment satisfy the same virial relationship as is obtained for the isolated atomic state, namely, that $-2\bar{T} = \bar{V}_e$. In terms of the present definitions this requires that

$$-2\bar{T}(A) = \bar{V}_A'(A) + \bar{V}_A''(A) \qquad (13)$$

where $\bar{V}_A'(A)$ is the attraction of nucleus A for the charge density in (A) and $\bar{V}_A''(A)$ is the self-repulsion of the electrons in (A). The satisfaction of eq 13 requires that the sum of all external contributions to the electronic virial of a fragment together with the nuclear virial vanish.

$$\sum_{\alpha} \mathbf{R}_\alpha \cdot \mathbf{F}_\alpha(A) + \bar{V}_B'(A) + \bar{V}_B''(A) = 0 \qquad (14)$$

Equation 13 or 14 is equivalent to requiring that the virials of all the forces resulting from the process of molecular formation vanish for a fragment. Table IV lists the total virials for a number of fragments ($2\bar{T}$(A)) together with $\Delta(A) = 2\bar{T}(A) + \bar{V}_A'(A) + \bar{V}_A''(A)$, a quantity which measures the extent by which the intrafragment fields deviate from the atomic virial relationship; *i.e.*, $\pm\Delta(A)$ are the errors in eq 13 and 14, respectively.[18]

The atomic virial relationship can be satisfied by a molecular fragment, as evidenced by (H) in the one-electron molecular-ion H_2^+ ($X\,^2\Sigma^+$, $R = 2.00$ au).[19] In this case, for which $\Delta\bar{V}''(A) = 0$, one finds the value of Δ(H) to be less than the error in the virial for the total system ($\Delta = 2T + V = 0.0098$ au). In general however, this is not the case and the values of Δ(A) and Δ(H) in Table IV indicate that the relative magnitudes of the internal fields of a fragment charge distribution are considerably changed from those of the isolated atomic or ionic state. The population of (Li) in LiH, for example, is very close to that of a Li^+ ion and its charge distribution is close to a spherical one. The small polarizations which are present, however, result in a decrease of 0.28 au in $\bar{V}_{Li}'$(Li) over the free ion value and an increase of 0.15 au in the electron–electron repulsions. It is interesting to note that if the repulsion of the (approximately) two electrons in (Li) did equal that found for the Li^+ ion, the atomic virial relationship would apply to this fragment.

Table IV. Satisfaction of Atomic Virial by Molecular Fragments

AH(X)	$2\bar{T}$(A)	Δ(A)	$2\bar{T}$(H)	Δ(H)
HH^+	0.6020	+0.0002	0.6020	+0.0002
HH	1.1261	+0.16	1.1261	+0.16
HeH^+	5.7654	+0.16	0.1016	+0.0079
LiH	14.7356	+0.15	1.2470	+0.17
BeH^+	28.2380	+0.35	1.4615	+0.37
BH	48.4578	+0.10	1.7748	+0.59

The errors Δ(A) and Δ(H) are positive in every case. This implies that the sum of the external electronic and nuclear virials is negative for every fragment and that the attractive forces exerted on a fragment by its neighbor are dominant.

In a previous paper[2] we have demonstrated that the charge distributions, average kinetic energies and thus the virials of the (H) fragments in BeH ($X\,^2\Sigma^+$) and BeH_2 ($X\,^1\Sigma^+$) are nearly identical. While the individual force contributions to the external virial of (H) from a localized nonbonded electron (in BeH) and a hydride ion (in BeH_2) are very different, their total contributions are nearly identical. The properties of BH_3, BF_3, BH_4^-, BH_3F^-, and BH_3CO are discussed in a forthcoming paper to further illustrate that the charge distribution and properties of a bonded fragment as defined by eq 1 remain unchanged in different bonding

---

(18) The value of $\bar{V}''$(A) is usually obtained indirectly *via* integration of the one-electron Hartree–Fock energy density expression.[1] Evaluation of $\bar{V}_A''$(A) requires direct integration of $\Gamma(\mathbf{x}_1,\mathbf{x}_2)$ over the volume of (A), a very time-consuming process. The values of Δ(A) in Table IV are given to two significant figures only as a consequence of the grid size employed in the evaluation of $\bar{V}_A''$(A).

(19) The wave function for H_2^+ is that of Guillemin–Zener using the parameters determined by S. Kim, T. Y. Chang, and J. O. Hirschfelder, *J. Chem. Phys.*, **43**, 1092 (1965).

environments to the extent that the external virials exerted by the neighboring fragments remain unchanged.[20] When a fragment does exhibit changes in its properties in different systems, *e.g.*, (B) in BH_3, BF_3, the changes may be directly related to changes in the electrostatic fields exerted on the fragment and the effect they have on its virial and charge distribution.

[20] R. F. W. Bader and G. Runtz, unpublished results.

Role of Charge Transfer Interactions in the Quenching of 1,4-Dimethoxybenzene Fluorescence[1,2]

Felix A. Carroll,[3] M. T. McCall,[4] and George S. Hammond*

Contribution No. 4422 from the Gates and Crellin Laboratories of Chemistry,
California Institute of Technology, Pasadena, California 91109.
Received February 8, 1972

Abstract: The fluorescence of 1,4-dimethoxybenzene (DMB) in acetonitrile is quenched by a number of organic compounds having lowest lying excited singlets higher in energy than that of DMB. The rate constants show a structure-reactivity pattern that seems to implicate charge transfer as an integral part of the quenching process. The group as a whole does not show a linear correlation of log k_q with quencher reduction potentials, even though a limited relationship of this kind appears in selected subseries. The results suggest that charge transfer provides the binding energy of the exciplex, while the internal conversion of electronic excitation involves a vibronic mechanism not strongly dependent on the reduction potentials of the quenchers.

The fluorescence of electronically excited molecules is often quenched by compounds having no excited singlet states lying low enough to be populated by transfer of electronic energy available in the quenchee. In particular, the quenching of naphthalene fluorescence by conjugated dienes,[5] aliphatic[6,7] and aromatic amines,[7] and strained hydrocarbons[8,9] has been investigated in our laboratory and in others.

The role of charge-transfer interactions in singlet quenching is still in dispute. We have suggested that while charge transfer is the dominant pathway of electronic deexcitation in the quenching of naphthalene fluorescence by aliphatic amines,[6] charge transfer is not entirely responsible for the quenching of naphthalene fluorescence by conjugated dienes.[5] Others, however, have concluded that charge transfer interactions are the source of fluorescence quenching in these cases as well.[10,11]

Recently we reported that the fluorescence of indole, *N,N*-diethylaniline, anisole, 2-methoxy- and 2,6-dimethoxynaphthalenes, and other "electron-rich" aromatic molecules was quenched by methyl chloroacetate and 2-chloroacetamide and that the ordering of quenching rate constants suggested charge transfer from the excited molecule to the quencher.[12] We have extended this study by determining the rate constants for the quenching of 1,4-dimethoxybenzene (DMB) fluorescence by several groups of organic compounds, and report results which yield additional insight into the quenching mechanism.

Experimental Section

Materials. Acetonitrile (Matheson Coleman and Bell, Spectroquality) was used as received. The 1,4-dimethoxybenzene (Aldrich) was recrystallized twice from hexane. Chloroacetonitrile (Matheson Coleman and Bell) and chloromethyl methyl ether (Aldrich) were distilled from phosphorus pentoxide and a center cut was taken. The benzyl acetates were synthesized by treating the corresponding benzyl alcohols (commercial materials) with acetic anhydride in pyridine; the products were distilled and a center cut was taken. Benzyl chloride (Matheson Coleman and Bell) and the para-substituted benzyl chlorides (Aldrich), allyl acetate (Eastman), allyl chloride (Matheson Coleman and Bell), and ethyl trifluoroacetate (Calbiochem) were distilled and center cuts were taken. Methyl chloroacetate was distilled twice; a center cut was taken each time. 2-Chloroacetamide was recrystallized twice from water. Acetic anhydride (Baker) and trifluoroacetic anhydride (Matheson Coleman and Bell) were used as received. The mesylates were prepared from the corresponding alcohols by the procedure of Hudson and Withey[13] except that the sodium hydroxide was omitted from the reaction mixture. Comparable yields were obtained. Allyl mesylate was vacuum distilled and benzyl mesylate was purified by bulb to bulb vacuum distillation. *p*-Chlorobenzyl mesylate, a solid, decomposed upon attempted vacuum sublimation. The material used was recrystallized repeatedly from 30:70 benzene: hexane and had a melting point of 48-53°.

Measurements. Relative fluorescence intensities were measured with an Aminco-Bowman spectrophotofluorometer. Samples were prepared in duplicate or triplicate in 13 × 100 mm Pyrex test tubes using 3-ml solutions of *ca.* 1.5×10^{-2} *M* DMB and varying concentrations of quencher. The tubes were degassed by three freeze pump thaw cycles at $\leq 5 \times 10^{-4}$ Torr.

---

[1] Mechanisms of Photochemical Reactions in Solution. LXXIV. For part LXXIII see F. A. Carroll and G. S. Hammond, *J. Amer. Chem. Soc.*, **94**, 7151 (1972).

[2] Presented in part at the Pacific Conference on Chemistry and Spectroscopy, Anaheim, Calif., Oct 1971. Abstract No. 148.

[3] National Science Foundation Predoctoral Fellow, 1969–present.

[4] National Institutes of Health Postdoctoral Fellow, 1969–1970.

[5] D. A. Labianca, G. N. Taylor, and G. S. Hammond, *J. Amer. Chem. Soc.*, **94**, 3679 (1972), and references therein.

[6] (a) S. P. Van, Ph.D. Thesis, California Institute of Technology, 1970; (b) M. G. Kuzmin and L. N. Guseva, *Chem. Phys. Lett.*, **3**, 71 (1969).

[7] D. Rehm and A. Weller, *Isr. J. Chem.*, **8**, 259 (1970), and references therein.

[8] S. Murov and G. S. Hammond, *J. Phys. Chem.*, **72**, 3797 (1968).

[9] G. N. Taylor, *Chem. Phys. Lett.*, **10**, 355 (1971).

[10] B. S. Solomon, C. Steel, and A. Weller, *Chem Commun.*, 927 (1969).

[11] T. R. Evans, *J. Amer. Chem. Soc.*, **93**, 2081 (1971).

[12] M. T. McCall, G. S. Hammond, O. Yonemitsu, and B. Witkop, *ibid.*, **92**, 6991 (1970).

[13] R. F. Hudson and R. J. Withey, *J. Chem. Soc. B*, 237 (1966).